AIAA JOURNAL
Vol. 47, No. 10, October 2009

Optical Characterization of a Simulated Weakly Compressible Shear Layer: Unforced and Forced

Alice M. Nightingale,* Stanislav Gordeyev,† and Eric J. Jumper‡
University of Notre Dame, Notre Dame, Indiana, 46556

DOI: 10.2514/1.34244

This paper uses a discrete-vortex code to examine a shear layer's response to forcing at its origin and to develop a relationship between a shear layer's optical characteristics and the commonly used characteristic growth length, vorticity thickness. The code and its thermodynamic overlay have been used in previous studies to predict the optically aberrating characteristics of relatively high-Mach-number, subsonic shear layers that can be classified as weakly compressible. A weighted-average natural frequency is introduced and used to characterize the unforced shear layer in terms of an optical characteristic length referred to as optical coherence length. It is shown that optical coherence length is related to vorticity thickness by a factor of approximately 3.18. The study also shows that the use of single-frequency forcing produces a regularized shear layer for distances preceding the point at which the unforced shear layer's natural frequency matches the forcing frequency. In the case of the forced shear layer, a greater thickness is produced closer to its point of origin until collapsing onto the unforced shear-layer thickness past the point of regularization. The aberration periodicity is shown to have lower robustness toward the furthest downstream extent of regularization due to uncontrolled pairing.

Nomenclature

A	=	aperture of laser beam, amplitude of forcing
C_δ	=	vorticity thickness growth rate constant
C_Λ	=	optical coherence length growth rate constant
f_f	=	forcing frequency
f_n	=	natural optical frequency
K_{GD}	=	Gladstone–Dale constant
n	=	index of refraction
R	=	velocity ratio
s	=	density ratio
U_c	=	convective velocity, $(u_U + u_L)/2$
u_L	=	lower freestream velocity in the x direction
u_U	=	upper freestream velocity in the y direction
x	=	streamwise or flow direction
y	=	normal direction to the plane of the shear layer, perpendicular to the main flow
δ_{vis}	=	shear-layer thickness
δ_ω	=	vorticity thickness
θ	=	momentum thickness
θ_j	=	jitter angle
Λ_n	=	optical coherence length
λ	=	dimensionless velocity ratio
ρ_L	=	lower stream density
ρ_U	=	upper stream density
ϕ	=	phase shift of forcing function

Received 3 September 2007; revision received 27 June 2008; accepted for publication 10 June 2009.

*Graduate Research Assistant, Aerospace and Mechanical Engineering Department, Center for Flow Physics and Control, Fitzpatrick Hall. Student Member AIAA.

†Research Assistant Professor, Aerospace and Mechanical Engineering Department, Center for Flow Physics and Control, Hessert Center. Member AIAA.

‡Professor, Aerospace and Mechanical Engineering Department, Center for Flow Physics and Control, Hessert Center. Fellow AIAA.

Introduction

WHEN an otherwise planar optical wave front is made to propagate through a relatively high-Mach-number, subsonic shear layer, the wave front becomes aberrated (see Fig. 1), adversely affecting its far-field intensity pattern. This degraded far-field intensity pattern is undesirable for use in optical systems. Although the optical characteristics of free shear layers have been investigated since the 1970s [1–3], it was only in the late 1990s that the cause of optical aberrations in shear layers was found to be the large-scale structures that naturally "roll up" [4]. More specifically, it was found that the radial pressure gradients, and associated density deficit required to support the curvature of the structure, were the cause of a large part of the optical aberrations [4]. For a Mach 0.8/0.1 shear layer, like the one experimentally investigated in [5,6], the aberrations approximately 0.5 m downstream from its point of origin are sufficient to reduce its far-field intensity by more than 80% of its otherwise unaberrated, diffraction-limited far-field intensity. These measurements were taken using a 1 μm laser beam given an aperture of at least a 20 cm [1].

It has long been known that placing a conjugate waveform on the optical wave front of a laser beam before its transmission through the aberrating medium results in the emergence of a planar-wave front beam as it leaves the medium (see Fig. 1). Systems that sense the aberration and construct and apply the proper conjugate waveform at regular time intervals are termed adaptive-optic (AO) systems [7].

A traditional AO system operates in consecutive steps, the first step being to sense the aberration for which a conjugate must be constructed. For projecting systems, the aberration of an incoming optical signal (or the remaining residual aberration after a correction has been made) at any given instant is measured using a wave front sensor (WFS). A conjugate constructor (CC), sometimes referred to as a reconstructor, then determines the distorted pattern necessary to make corrections. Although the rate at which the CC is able to convert wave front measurements into command signals is important, in general the CC is typically much faster than the WFS and, at present, does not form the bandwidth-limiting step. This conjugate (or some portion of it; see Fig. 1b) is then sent to a deformable mirror (DM), for which the electromechanical character, including its source of excitation (i.e., amplifiers), limits the rate at which it can respond to signals adjusting its figure. The conjugate wave front is placed on the laser before its propagation through the aberrating turbulence by first reflecting it off the DM (see Fig. 1b).

In the traditional approach, the control system is a feedback system that forms another bandwidth-limiting step/component in the AO

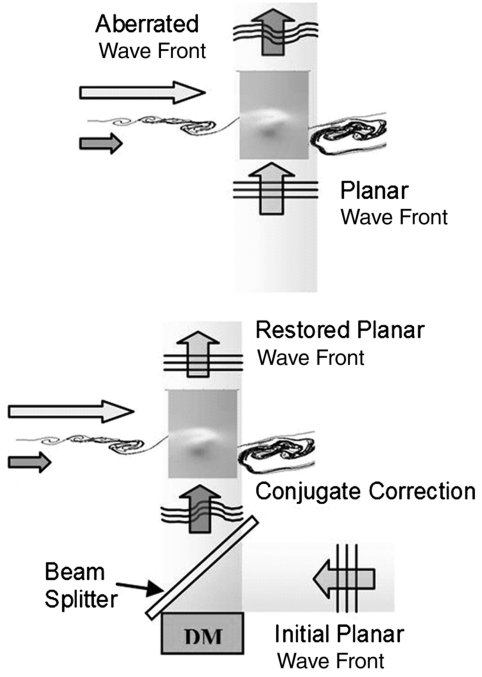

Fig. 1 Shown are the following: a) planar-wave front propagated through a turbulent shear-layer flow and emerging aberrated, and b) the effect of placing a conjugate correction on the beam before propagation.

system. This last step has been extensively studied by Tyson [7] and others. Typically only $\sim 1/10$th of the residual error can be removed for each DM update (usually the clock time of the WFS) to keep feedback approaches stable. This update rate is often referred to as the system gain, 0.1 in this case. On the other side of the equation is the bandwidth requirement set by the aberrating flowfield itself. As described in Tyson [7] and reexamined and affirmed specifically for aero-optic disturbances by Cicchiello and Jumper [2], an aberration must be removed approximately 10 times per its aberration-coherence-length clearing time to restore 80% of its diffraction-limiting performance. This means that assuming a system gain of 0.1 and that the system-limiting component is the wave front sensor for an aberrating flow that initially reduces the Strehl ratio to less than 0.1, for a traditional AO approach, in which an aberration has a clearing frequency through the aperture of 1 kHz, the wave front sensor must frame at 100 kHz in real time to restore an 80% Strehl ratio. The fastest real-time wave front sensors that exist today operate at an order of magnitude lower than this. Even if a real-time wave front sensor of this speed were available, other components in the AO system would form a barrier to correcting a 1 kHz aberration, yet the aberrations posed by a high-Mach subsonic shear layer are at least 1 kHz [8–12].

Realizing that such bandwidth requirements make traditional approaches unrealistic, this paper explores the beginning stages of an alternative approach to performing adaptive-optic corrections of a laser propagating through a high-speed subsonic shear layer. The end goal will be to use flow control to "regularize" the shear layer's aberrating character, effectively reducing the bandwidth requirements necessary to perform adaptive-optic corrections. Two separate experiments performed at Notre Dame, with a forced heated jet and a forced shear layer, have been conducted showing successful adaptive-optic corrections of the emerging laser using an open-loop phasing technique [9]. In a less contrived manner, a control system will be required to perform this optimization in real time without resorting to open-loop, manual amplitude, and phase adjustments. To develop the required control system, it will be necessary to develop models of each component in the system, including the shear layer itself and its optical response to forcing.

The results shown in this paper were obtained using a discrete-vortex-based code referred to as the "weakly compressible model" (WCM). Developed by Jumper and Hugo [11] and Hugo [13] and improved by Fitzgerald and Jumper [4] and Fitzgerald [14], this code was first used to develop wave front sensors and later to discover the physics of the aberrating mechanism in a matched-total-temperature shear layer [4]. The weakly compressible model has been shown to closely match the optical response of an unforced shear layer [12,15]. This paper describes the first steps in performing system identification of a shear layer's response to forcing using the weakly compressible model. The paper will give a brief description of the code and a review of comparisons between the code's unforced characteristics and those of the experimental shear layers. Subsequently, a measure of the shear layer's optical characteristics will be defined. In particular, a relationship between a shear layer's optical response and more-traditional measures of a shear layer's fluid-mechanic structure found in the literature will be established. Finally, the shear layer's response to forcing will by analyzed in terms of its optical character.

Weakly Compressible Model

A detailed description of the weakly compressible model discrete-vortex-based code can be found elsewhere [4]; however, a brief description of its underlying components will be given here. The code uses a two-dimensional discrete-vortex method to compute the velocity field for a free shear layer that originates at a splitter plate; it has been used to simulate shear layers with high-speed sides up to Mach 1.0 [15]. In even the highest-speed cases, the convective Mach numbers were less than 0.45 and, as discussed in Fitzgerald and Jumper [4], such shear layers are referred to as weakly compressible, making incompressible approaches to predicting the velocity field only slightly in error when neglecting the dilitation terms [4,16]. The unsteady velocity field resulting from the discrete-vortex method forms the basis for computing the thermodynamic properties. The thermodynamic properties are found by overlaying the momentum and energy equations (along with an isentropic estimate of total temperature variation) onto the velocity field by first back solving for an initial estimate of the pressure field. Iterative corrections for the temperature and density fields are then performed until a self-consistent field of thermodynamic properties is converged upon. Once the converged density field is known at each time step, the density is converted to an index of refraction using the Gladstone–Dale constant.

As described in [4], the largest contributor to the optical aberrations in the shear layer is the formation of coherent structures in the shear layer under the influence of the Kelvin–Helmholtz instability. In the convecting frame, these coherent structures form vortices with diameters that roughly match the vorticity thickness of the shear layer and contain high flow curvature. This curvature gives rise to concomitant pressure gradients that in turn give rise to relatively deep low-pressure cells or "wells" within the vortices accompanied by drops in the local density. Local regions of higher pressure and density that form in the local stagnation regions or saddle points along the braids between vortices (in the convecting frame) also contribute to the aberrating character of the shear layer. The most controversial part of this explanation for the physics of the shear layer's aberrating character was the notion that relatively deep pressure wells could form in a shear layer, because the prevailing thought at the time was that static-pressure fluctuations in a shear layer were negligible, based on the so-called strong Reynolds analogy [4]. However, experiments performed to investigate fluctuating pressure showed that the actual pressure wells measured in these vortices closely matched the predictions of the weakly compressible model [12]. The optical character was also shown to closely match the predictions of the weakly compressible model [12]. Figure 2 gives selected results from these comparisons. Extensive comparisons of the discrete-vortex code with experiments have been reported elsewhere as well. Among these is the comparison of the amplification of disturbances input at the splitter plate to the theoretical linear-stability amplification factors. These latter comparisons showed good agreement with theory, which itself has been shown to be in good agreement with experiments [4,13,14].

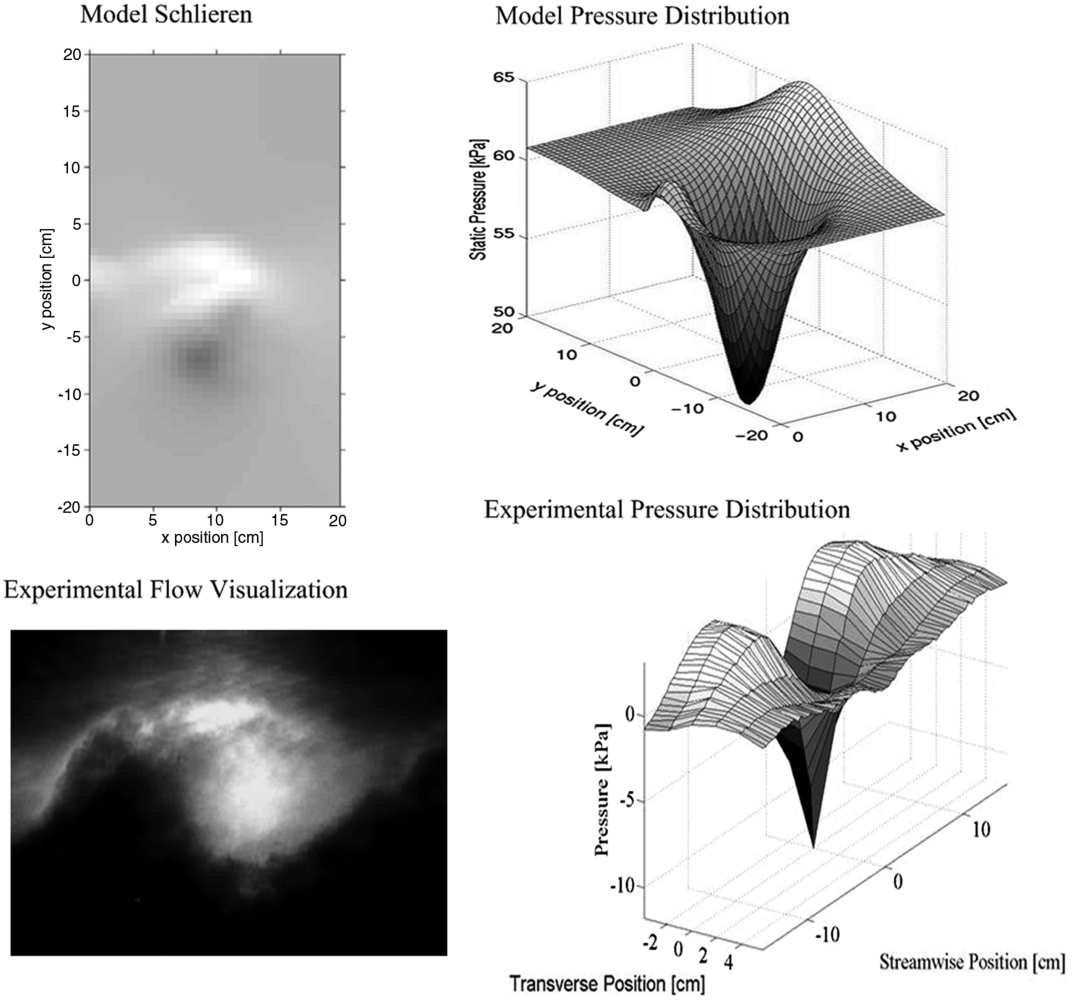

Fig. 2 Comparison: a, b) predictions of the weakly compressible model [4], and c, d) experiment [11,12].

This paper uses results obtained from the weakly compressible model to investigate the relationship between a shear layer's vorticity thickness and its optical characteristics. An analysis of the shear layer's response to forcing is also presented.

Characteristics of Unforced Shear Layers

In general, most experimental studies characterize a shear layer in terms of its thickness measure, the most common of which is either the shear layer's vorticity thickness, δ_ω, or the shear layer's momentum thickness, θ, given, respectively, by

$$\delta_\omega = \frac{u_U - u_L}{\left(\frac{\partial u}{\partial y}\right)_{\max}} \tag{1}$$

and

$$\theta = \int_{-\infty}^{+\infty} \frac{u(y) - u_L}{u_U - u_L}\left(1 - \frac{u(y) - u_L}{u_U - u_L}\right) \mathrm{d}y \tag{2}$$

where $u(y)$ represents the streamwise velocity component as a function of vertical location, y, for a given downstream location. These two measures are approximations of the on-average structure size in the vertical or normal direction to the plane of the shear layer. Although highly turbulent, on average a shear layer experiences a linear growth rate in terms of its vorticity thickness and momentum thickness due to the pairing/amalgamation process undergone by the large-scale vortical structures convecting downstream. Extensive experimental studies of shear layers with convective Mach numbers of less than ~0.45 were performed by Brown and Roshko [3], who were among the first to predict a shear layer's growth rate by

$$\frac{\delta_\omega}{x} = C_\delta \frac{(1-R)(1+s^{\frac{1}{2}})}{(1+Rs^{\frac{1}{2}})} \tag{3}$$

where $R = u_L/u_U$, $s = \rho_L/\rho_U$, and $C_\delta = 0.085$. Several simulations with varying convective velocities and velocity ratios were performed comparing the weakly compressible model results to the corresponding predicted growth rate based upon Eq. (3) (see Table 1) given an assumed density ratio, s, of 1.0. Figure 3 shows the vorticity thickness versus downstream distance for a free shear layer with an upper freestream velocity of 261.04 m/s, and a lower freestream velocity of 34.7 m/s simulates the flowfield experimentally studied in [5,6]. The numerically computed vorticity thickness (shown by the triangles in Fig. 3) has an approximate growth rate of 0.131, closely resembling the predicted growth rate from Eq. (3) of 0.130, where $R = 0.13$ and $s = 1.0$ (shown by a solid line in Fig. 3). It should be noted that the DVM often overpredicts shear-layer growth rates for actual gas flows at the speeds simulated [5]; however, it still provides considerable insight into the flowfield characteristics assuming a density ratio of 1.0.

The thermodynamic properties, including time-dependent density fields, were then computed from the series of velocity fields and used to determine the effect of a laser propagating through the shear layer. In each of the computations referred to in this paper, a series of approximately 8000 time steps was run, with approximately 33 μs between time steps. Simulations were performed using an initial vortex core size of 0.01725 m and a rectangular velocity grid spacing in both the x and y directions of 0.005 m. A simulated beam with an aperture of 0.25 m was swept along the x direction (propagated perpendicularly through the flowfield) to the obtain optical path length and optical path difference measures [see Eqs. (4) and (6) for their definitions]. The following section derives another thickness

Table 1 Numerical and analytical characteristics with corresponding convective velocities and velocity ratios ($s = 1.0$)

U_c, m/s	R	$\Delta\Lambda_n/\Delta x$	$\Delta\delta_\omega/\Delta x$
106	0.06	0.42	0.15
147.9	0.08	0.43	0.15
147.9	0.13	0.37	0.13
148.5	0.15	0.32	0.12
117.5	0.18	0.33	0.12
127.5	0.19	0.30	0.11
147.9	0.28	0.25	0.09
117.5	0.31	0.22	0.09

measure in terms of the shear layer's optical characteristics. The goal of this analysis is to provide a means of characterizing a shear layer's optical properties and link those back to the commonly used vorticity thickness measure defined earlier.

Optical Response of the Shear Layer

As described in [4], the index-of-refraction fields are sufficiently weak that a simple integration through the field in the y direction can be used to compute the optical path length (OPL) as a function of position and time:

$$\mathrm{OPL}\,(x,t) = \int_{y_1}^{y_2} n(x,y,t)\,\mathrm{d}y \tag{4}$$

where the index of refraction is related to the density by

$$n(x,y,t) = 1 + K_{\mathrm{GD}}\rho(x,y,t) \tag{5}$$

The optical path difference, $\mathrm{OPD}(x,t)$, may then be computed by removing the spatially averaged OPL over the aperture from the local OPL according to

$$\mathrm{OPD}_A(x,t) = \mathrm{OPD}(x,t) - \overline{\mathrm{OPD}}_A(x,t) \tag{6}$$

producing a wave front that is advanced or retarded as a function of x from the mean phase over the aperture. The optical wave front is defined as the locus of points along which the beam's phase is constant. It can be shown [13] that the displacement of the wave front from the mean at an instant in time, t, has the conjugate value of the OPD(x,t). Because of this, it is common for the wave front to be described as the OPD.

According to Huygens's principle, a wave front will propagate in a direction normal to itself. Concomitantly, a small-aperture laser beam initially normal to an incoming laser's wave front, directed through an aberrating flowfield in the y direction, will emerge normal to the outgoing aberrated wave front [10] at an angle, $\theta_j(x,t)$, defined as

$$\theta_j(x,t) = \arctan\left(-\frac{\mathrm{dOPD}(x,t)}{\mathrm{d}x}\right) \tag{7}$$

When a small-aperture beam is projected through an experimental turbulent flowfield, its emerging angle, $\theta_j(x,t)$, can be recorded at high rates exceeding 100 kHz. This time series of angles is referred to as the beam's "jitter." The results in Figs. 4 and 5 were obtained by numerically propagating small-aperture laser beams through the flowfield at several locations downstream from the splitter plate. Time-varying jitter signals were obtained from the weakly compressible model by calculating a time series of the OPD from the density field using Eqs. (4–6) and computing jitter angles using Eq. (7).

The frequency content of the jitter signal is clearly related to the coherent structures in the shear layer [4] and, as such, contains information about the coherence lengths of the aberrating structures convecting through the beam. Figure 4 shows the power spectral density (PSD) of the jitter signals at selected downstream locations from the splitter plate. A mean or "natural optical frequency" at each x location was computed from the PSDs according to

$$f_n(x) = \frac{\int \mathrm{PSD}(f,x)\; f\; \mathrm{d}f}{\int \mathrm{PSD}(f,x)\; \mathrm{d}f} \tag{8}$$

where the n subscript on f indicates the "natural," unforced optical frequency in the shear layer at the particular x location. Figure 5 shows a plot of the natural optical frequency versus the distance from the splitter plate. It should be noted that Eq. (8) provides a means of calculating the average frequency versus the downstream distance based upon numerical data. Therefore, when applying this method to experimental data, great care must be taken in filtering out any

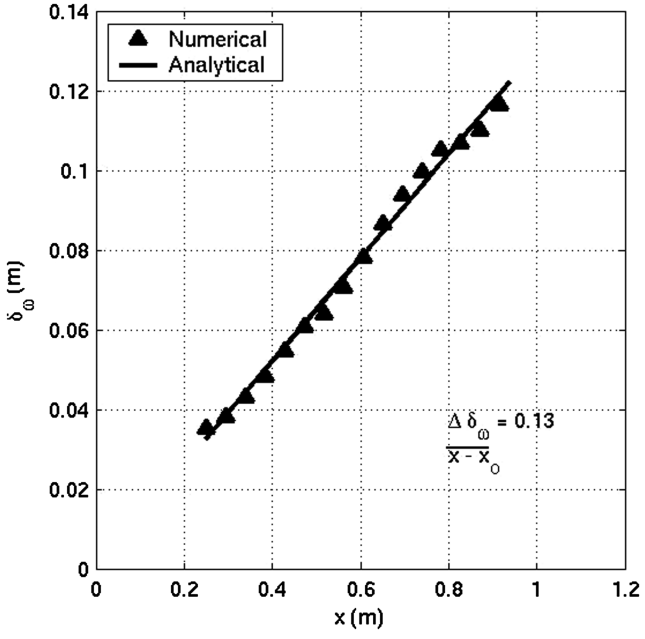

Fig. 3 Vorticity thickness versus downstream distance for an unforced shear layer, where $u_U = 261.04$ m/s and $u_L = 34.7$ m/s.

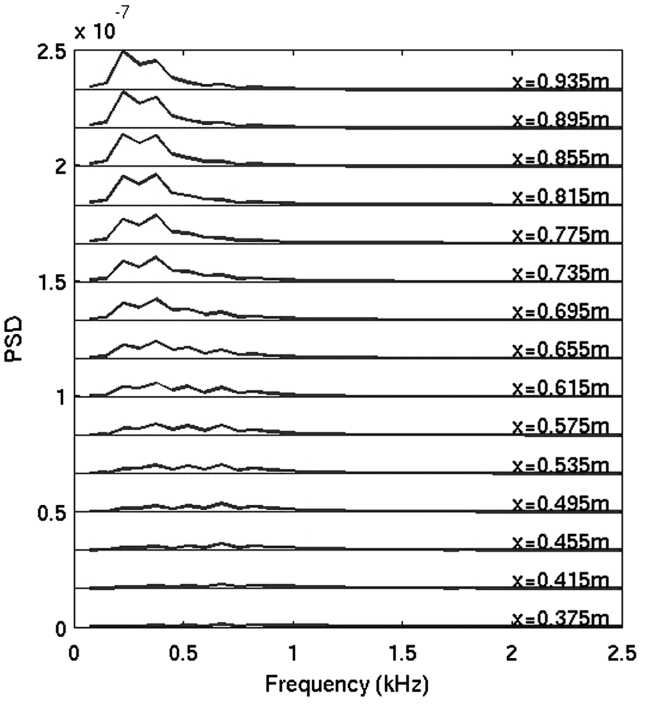

Fig. 4 Average PSD for numerically flow-induced jitter angles at various locations downstream from the splitter plate, where $u_U = 261.04$ m/s and $u_L = 34.7$ m/s.

frequencies not associated with the shear-layer dynamics themselves [6]. The results displayed in Figs. 4 and 5 were obtained using a numerical sample rate of approximately 33 μs. At each x location, the PSD was calculated by averaging 20 different data sets, each containing a series of 2048 consecutive time steps. The PSD plots and averaged natural optical frequencies for a given set of flowfield conditions are shown in Fig. 4.

As mentioned earlier, these frequencies can be related to an average optical coherence length by dividing the convection velocity by the natural optical frequency:

$$\Lambda_n(x) = U_c / f_n(x) \tag{9}$$

As each coherent vortical structure passes through one of the small-aperture lasers, the beam undergoes one full cycle of beam jitter corresponding to one full wavelength of optical coherence length [13]. This means that optical coherence length, as defined in Eq. (9), is a measure of the statistical on-average streamwise size of large-scale vortical structures passing through the laser beam (i.e., spacing between large-scale structures). Figure 6 shows a plot of the optical coherence length versus downstream distance from the splitter plate.

Similar to vorticity thickness (Fig. 3), which provides a measure of the shear layer's thickness in the vertical/normal direction, the unforced shear-layer structures also experience a linear growth rate in the streamwise direction. However, when comparing Figs. 3–6, a difference between the growth rate values in these two directions is evident. This particular shear-layer case produces a numerical optical coherence growth rate of 0.37 compared with a numerical vorticity thickness growth rate of 0.131. Several shear-layer cases were simulated with varying upper and lower stream velocities to further investigate this difference in growth rates. Each case was simulated using a rectangular grid with 0.005 m spacing in the x and y directions. Time averaging was calculated using a sample size of approximately 8000 time steps given an approximate time step of 33 μs. Each jitter signal was evaluated at a single location in space, simulating an "infinitesimal" small-aperture beam. Time-averaged vorticity thicknesses and time-averaged optical coherence lengths were numerically computed to determine the relationship between these two measures of structure size. Figure 7 shows a plot of the numerical vorticity thickness growth rate versus numerical optical coherence length growth rate. A linear fit was used to determine the

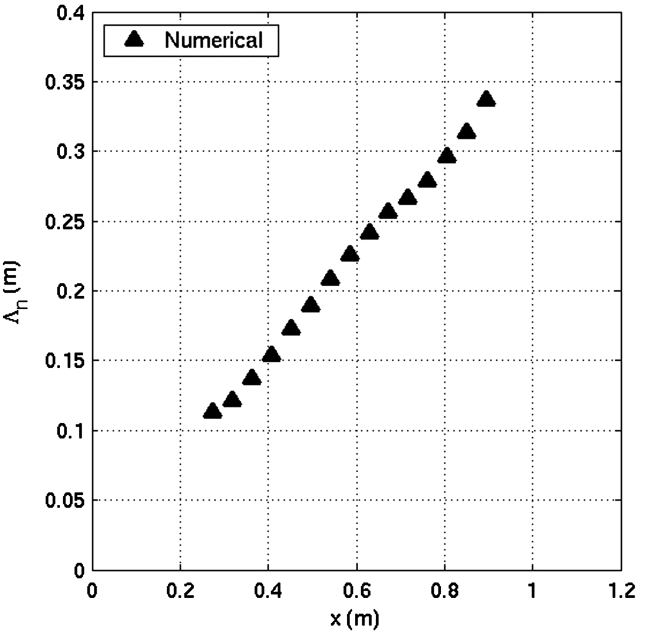

Fig. 6 Optical coherence length versus downstream distance for an unforced shear layer, where $u_U = 261.04$ m/s and $u_L = 34.7$ m/s.

factor relating these two shear-layer measures, for which the norm of the residuals was approximately 0.026.

As seen in Fig. 7, the unforced shear-layer structures grow at a rate approximately 3.18 times greater in the streamwise direction as compared with the normal direction. Therefore, the optical coherence length closely defines the measure of vorticity thickness, with a factor of 3.18 being the relationship between the coherence length in the x direction (related to vortex spacing) and the shear-layer thickness in the normal, or y, direction (related to vortex size). It is important to notice that this factor of 3.18 is larger than the factor of 1.5–2.0 found in Brown and Roshko [3], who described the relationship between coherent-structure scale size, δ_ω, in a shear layer and the visual shear-layer thickness, δ_{vis}. This difference is attributable to fact that the natural optical frequency defined in Eq. (8) is essentially a measure of the vortex spacing in the x direction rather than the visual shear-layer thickness. The factor of 3.18 agrees with results given in [3,8], in which it is noted that a shear layer's large-scale structures are typically spaced a distance of approximately 3 times the shear layer's thickness at each respective x location.

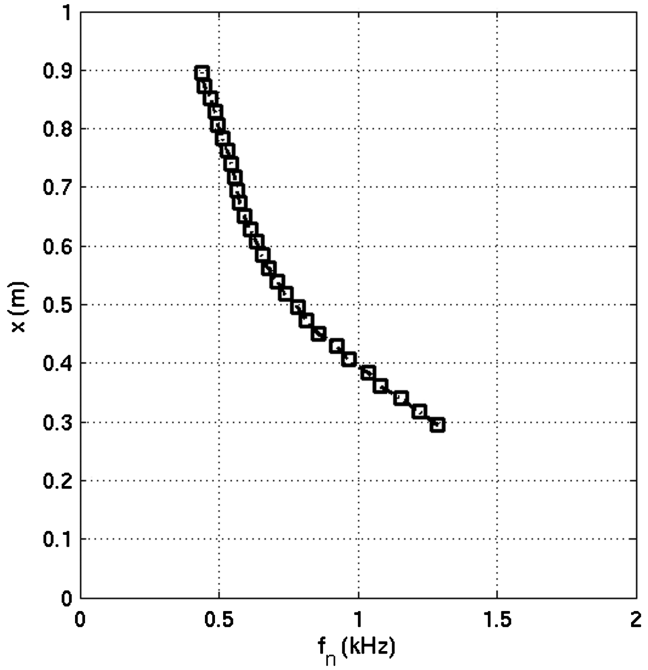

Fig. 5 Downstream distance, x, from the splitter plate versus natural optical frequency, f_n, for an unforced shear layer, where $u_U = 261.04$ m/s and $u_L = 34.7$ m/s.

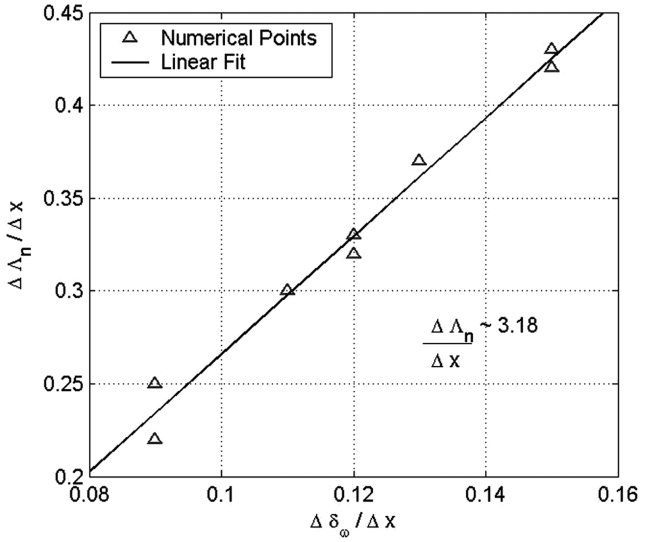

Fig. 7 Numerically computed optical coherence length growth rate versus vorticity thickness growth rate given varying upper and lower stream velocities.

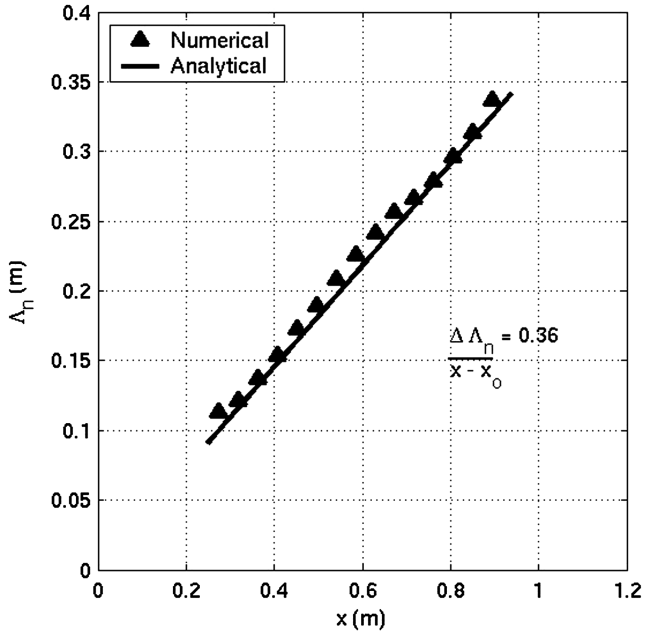

Fig. 8 Natural coherence length versus downstream distance for an unforced shear layer, where $u_U = 261.04$ m/s and $u_L = 34.7$ m/s.

The results shown in Fig. 7 are listed in Table 1 along with their respective convective velocities and velocity ratios. On average, both the optical coherence length growth rate and the vorticity thickness growth rate increase as the ratio of lower stream velocity to upper stream velocity decreases. In other words, as the difference in velocity between the upper and lower streams increases, so do the rates at which the large-scale structures grow, as well as the spacing between them.

Although a density ratio, s, of 1.0 has been assumed throughout this numerical study, it seems reasonable that the form of the well-established vorticity thickness growth rate equation [Eq. (3)] [3,17], would also be relevant for optical coherence length growth rates. Therefore, optical coherence growth rate may be predicted by

$$\frac{\Lambda_n}{x} = C_\Lambda \frac{(1-R)(1+s^{\frac{1}{2}})}{(1+Rs^{\frac{1}{2}})} \tag{10}$$

where the new constant, C_Λ, is equal to 0.27 (this value was obtained by multiplying the vorticity thickness constant [3] by the scaling factor of 3.18 derived earlier). As already noted, the DVM commonly overpredicts a shear layer's growth rate; therefore, a numerical correction factor is needed to compare the analytical optical coherence length growth rate [Eq. (10)] with the numerically computed growth rates. A correction factor of 0.86 was computed based on the numerical results given in Table 1 and the analytically calculated growth rates using Eq. (10) (assuming a density ratio of 1.0). Applying this correction factor to Eq. (10), the predicted optical coherence length for the shear-layer case studied earlier (Fig. 6) was computed and plotted against the numerically computed growth rate. Figure 8 shows good correspondence between the analytical optical coherence growth rate of 0.36 and the numerical optical coherence growth rate of approximately 0.37.

For applications in which optical (nonintrusive) measuring techniques are more appropriate, optical coherence length provides a means of analyzing and characterizing the shear layer's flow dynamics. It also affords a link between the commonly used thickness characteristics and optical characteristics of the shear layer. Such a relationship becomes beneficial when analyzing the optical response of a shear layer to forcing described in the following section.

Response of the Weakly Compressible Model to Forcing

A recent numerical study by Freund and Wei [18] and an experimental investigation by Rennie et al. [19] showed that the most effective means of forcing a shear layer is to displace the edge of the splitter plate in the direction normal to its surface. In the case of the discrete-vortex code, forcing was simulated by inserting the first vortex into the shear layer displaced from the splitter-plate edge in the vertical, y, direction by an amount

$$d(t) = A \sin(2\pi f_f t + \phi) \tag{11}$$

A range of frequencies and amplitudes were applied to several different shear-layer cases to establish the response of a shear layer to forcing as predicted by the weakly compressible model.

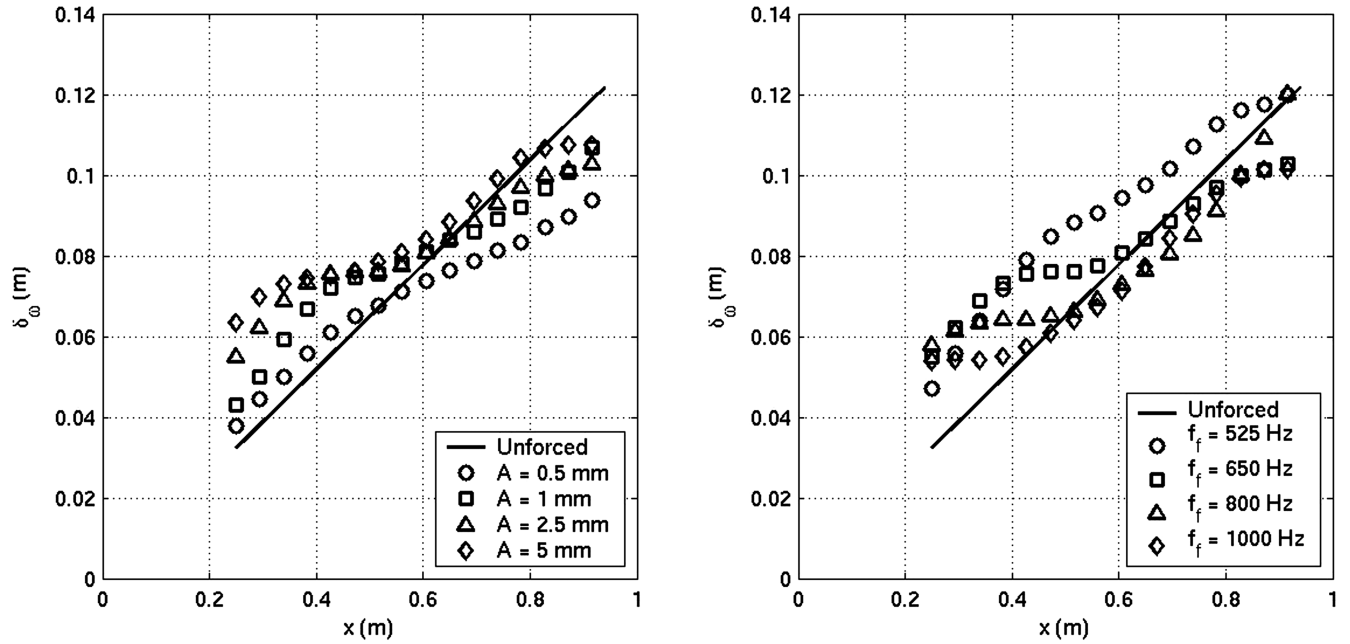

Fig. 9 WCM predictions of vorticity thickness versus downstream distance for a forced shear layer with an upper stream velocity of $u_U = 261.04$ m/s and a lower stream velocity of $u_L = 34.7$ m/s: a) results for a shear layer forced at a frequency of $f_f = 650$ Hz with varying forcing amplitudes, and b) results for a shear layer forced at varying frequencies with an amplitude of $A = 2.5$ mm.

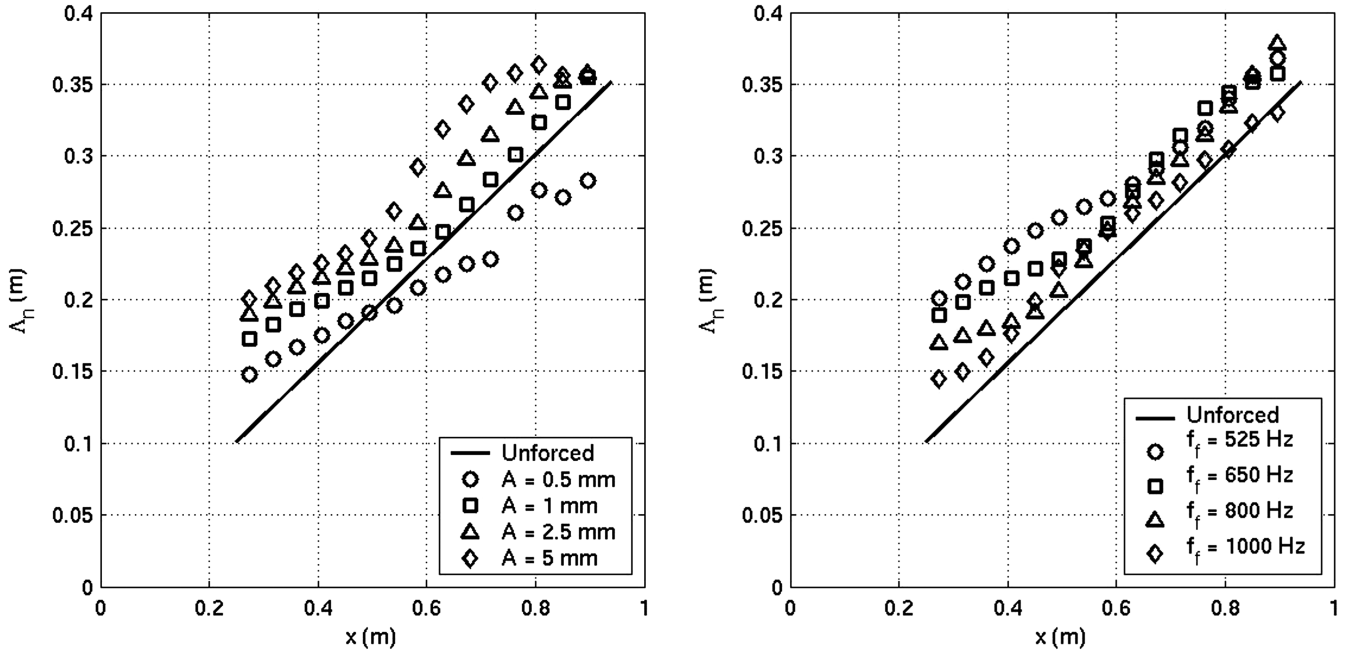

Fig. 10 WCM predictions of optical coherence length versus downstream distance for a forced shear layer with an upper stream velocity of $u_U = 261.04$ m/s and a lower stream velocity of $u_L = 34.7$ m/s: a) results for a shear layer with $f_f = 650$ Hz with varying forcing amplitudes, and b) results for a shear layer forced at varying frequencies with $A = 2.5$ mm.

Figures 9 and 10 each show two plots of the effect of forcing in terms of vorticity thickness and optical coherence length, respectively. The vorticity thickness versus downstream distance for a shear layer forced with a range of amplitudes given a constant forcing frequency, $f_f = 650$ Hz, is shown in Fig. 9a, and the shear layer forced with varying frequencies while maintaining a fixed amplitude, $A = 2.5$ mm, is shown in Fig. 9b [per Eq. (11)]. The obvious effect of forcing is to abruptly increase the shear layer's growth rate and then "stabilize" its thickness for a region preceding the position at which the shear-layer thickness would have been in the unforced case; at this point the forced shear layer begins growing at a rate similar to the unforced shear layer. The shear layer's spreading rate is therefore slightly suspended before pairing and continuing to spread again. Increasing the forcing amplitude moves the sudden thickening of the shear layer, related to the structure roll up, closer to the splitter plate. This is in agreement with previous research studies that measured the growth of shear layers under the influence of forcing [8,18]. In an experimental study performed by Wygnanski and Oster, similar trends were observed for a forced mixing layer [20]; increasing the forcing amplitude resulted in an earlier and more robust stabilization of the mixing layer, and decreasing the forcing frequency moved the region of regularization further downstream.

Figure 10 shows the optical coherence length versus downstream distance for the same set of varying forcing conditions. It is clear that the information contained in Figs. 9 and 10 displays similar trends. The obvious difference is that the vorticity thickness shows a flatter slope in the "region of regularization" than the optical coherence length. This is due to the fact that, as the structures evolve and convect, the spacing between them grows slightly in the flow direction while retaining approximately the same thickness in the y direction, thus causing the optical coherence length to maintain a slight increase with downstream distance in the regularized region. This can be seen more clearly when studying plots of the shear-layer loci, the locus of points indicating the locations of the discrete vortices that define the undulation of the shear layers "contact surface." Figure 11 shows two such plots of the shear-layer loci, one for the unforced shear layer shown in Fig. 11a and the other for the forced shear layer shown in Fig. 11b.

The results displayed in Figs. 9–11 also agree well with Wygnanski and Oster's prediction of a mixing layer's spatial extent of regularization. In [20], a regularized region, delineated by an array of quasi-two-dimensional large-scale vortices that do not interact with one another, is defined by the locations, x, satisfying the following inequality:

$$1 < (\lambda f_f / U_c)x < 2 \tag{12}$$

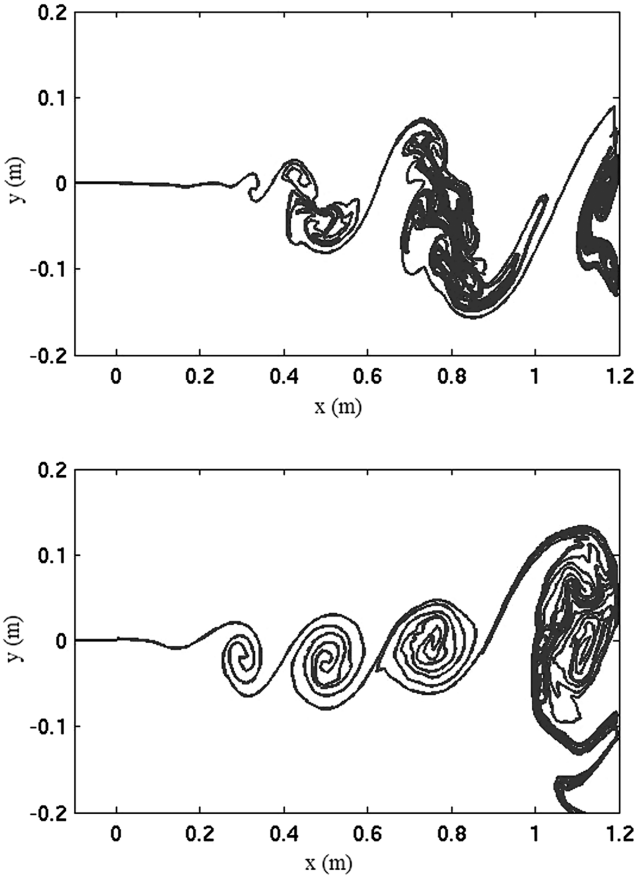

Fig. 11 Single realization of a shear-layer loci simulated using the weakly compressible model: a) unforced, and b) forced at 650 Hz with an amplitude of 2.5 mm.

where λ is a dimensionless velocity ratio defined as

$$\lambda = (u_U - u_L)/(u_U + u_L) \tag{13}$$

Given the set of parameters simulated in Figs. 9–11, in which the forcing frequency is equal to 650 Hz, Eq. (12) predicts a regularized region between 0.3 and 0.6 m downstream from the splitter plate. This prediction corresponds well with the region of regular coherent large-scale structures shown in Fig. 11. The optical coherence length provides a very useful characterization of the shear layer's growth rate in terms of its optical properties. It also aids in the selection of the appropriate forcing frequency necessary to regularize a specified region within the shear layer.

Conclusions

Numerical two-dimensional high-Mach-number subsonic shear layers and related optical aberrations were studied using a discrete-vortex method coupled with the weakly compressible model. The model was shown to qualitatively and quantitatively match experimentally observed shear-layer evolution and, hence, used to study the optical characteristics of the unforced and forced free shear layer. The results reported in this paper demonstrate that optical interrogation of a variable-index-of-refraction shear layer yields similar information to other methods of documenting the shear layer's characteristics. Optical coherence length, a statistical measure of the on-average large-scale structure size in the streamwise direction, showed a linear growth rate of approximately 3.18 times that of the vorticity growth rate. This factor agrees with previously reported vortex spacing discussions. Because a linear relationship exists between the shear layer's vorticity thickness, δ_ω, and its optical coherence length, Λ_n, optical measurements provide a nonintrusive means of measuring the shear layer's local structure size in the x direction and could be useful when intrusive ways of measuring thickness are difficult or impossible, as in chemically or thermally hostile environments (jet-engine exhaust, for example).

This numerical study demonstrated that it is possible to regularize a high-Mach-number subsonic shear layer through forcing, corroborating with previously run experimental investigations. In agreement with previously published studies, the forced shear layer was shown to experience an increased growth rate early on, until a region of stabilized growth was achieved. Within this region of regularization, large-scale coherent structures retain a relatively constant vertical/normal size while slightly growing in the streamwise direction. As the structures convect downstream, a pairing or merging process is eventually undergone, at which point the forced shear layer begins growing at a rate similar to the unforced case. Stabilizing the fluid mechanics of the shear layer also regularized its optical characteristics.

This study was performed specifically to investigate the applicability of using flow control to regularize the shear layer and its optical characteristics, with the goal of determining an estimation model of the emerging aberrated wave front. Such an estimation model would be used in an alternative AO approach, in which a prediction of the wave front aberrations would be "fed forward" and synchronized with the actual shear-layer-induced aberrations using a phase-locked-loop feedback control scheme.

Acknowledgments

These efforts were sponsored by the U.S. Air Force Office of Scientific Research, Air Force Material Command, U.S. Air Force, under grant FA9550-06-1-0160. The U.S. Government is authorized to reproduce and distribute reprints for governmental purposes notwithstanding any copyright notation thereon. The authors are grateful to the Directed Energy Professional Society for their support as well as to Bill Goodwine for his role as a coadvisor.

References

[1] Cicchiello, J. M., Fitzgerald, E. J., and Jumper, E. J., "Far-Field Implications of Laser Transmission through a Compressible Shear Layer," *Free-Space Laser Communication Technologies XIII Conference*, Vol. 4272, Society of Photo-Optical Instrumentation Engineers, Bellingham, WA, Jan. 2001, pp. 245–259.

[2] Cicchiello, J. M., and Jumper, E. J., "Far-Field Optical Degradation Due to Near-Field Transmission through a Turbulent Heated Jet," *Applied Optics*, Vol. 36, No. 25, 1997, pp. 6441–6452. doi:10.1364/AO.36.006441

[3] Brown, G. L., and Roshko, A., "On Density Effects and Large Structure in Turbulent Mixing Layers," *Journal of Fluid Mechanics*, Vol. 64, No. 4, 1974, pp. 775–816. doi:10.1017/S002211207400190X

[4] Fitzgerald, E. J., and Jumper, E. J., "The Optical Distortion Mechanism in a Nearly Incompressible Free Shear Layer," *Journal of Fluid Mechanics*, Vol. 512, Aug. 2004, pp. 153–189. doi:10.1017/S0022112004009553

[5] Hugo, R. J., Jumper, E. J., Havener, G., and Stepanek, S. A., "Time-Resolved Wavefront Measurements Through a Compressible Free Shear Layer," *AIAA Journal*, Vol. 35, No. 4, April 1997, pp. 671–677.

[6] Fitzgerald, E. J., and Jumper, E. J., "Aperture Effects on the Aero-Optical Distortions Produced by a Compressible Shear Layer," *AIAA Journal*, Vol. 40, No. 2, Feb. 2002, pp. 267–275. doi:10.2514/2.1668

[7] Tyson, R. K., *Principles of Adaptive Optics*, Academic Press, San Diego, 1991.

[8] Ho, C.-M., and Huerre, P., "Perturbed Free Shear Layers," *Annual Review of Fluid Mechanics*, Vol. 16, Jan. 1984, pp. 365–424. doi:10.1146/annurev.fl.16.010184.002053

[9] Duffin, D. A., "Feed-Forward Adaptive-Optic Correction of Aero-Optical Aberrations Caused by a Two-Dimensional Heated Jet," AIAA Paper 2005-4776, June 2005.

[10] Jumper, E. J., and Fitzgerald, E. J., "Recent Advances in Aero-Optics," *Progress in Aerospace Sciences*, Vol. 37, No. 3, April 2001, pp. 299–339. doi:10.1016/S0376-0421(01)00008-2

[11] Jumper, E. J., and Hugo, R. J., "Quantification of Aero-Optical Phase Distortion Using the Small-Aperture Beam Technique," *AIAA Journal*, Vol. 33, No. 11, 1995, pp. 2151–2157. doi:10.2514/3.12960

[12] Chouinard, M., Asghar, A., Kirk, J. F., Siegenthaler, J. P., and Jumper, E. J., "An Experimental Verification of the Weakly-Compressible Model," AIAA Paper 2002-0352, Jan. 2002.

[13] Hugo, R. J., "Quantifying the Spatio-Temporal Effects of Optically-Active Turbulent Flowfields on a Coherent Optical Wave," Ph.D. Dissertation, Aerospace and Mechanical Engineering Dept., Univ. of Notre Dame, Notre Dame, IN, April 1995.

[14] Fitzgerald, E. J., "The Shear Layer Compressibility Mechanism and its Role in Creating Aero-Optical Distortions," Ph.D. Dissertation, Aerospace and Mechanical Engineering Dept., Univ. of Notre Dame, Notre Dame, IN, 2000.

[15] Fitzgerald, E. J., Siegenthaler, J. P., and Jumper, E. J., "Optical Characterization of the Notre Dame Compressible Shear-Layer Facility," AIAA Paper 2002-2274, May 2002.

[16] Eldredge, J. D., Colonius, T., and Leonard, A., "A Dilating Vortex Particle Method for Compressible Flow," *Journal of Turbulence*, Vol. 3, No. 36, 2002, pp. 1468–5248.

[17] Dimotakis, P. E., "Two-Dimensional Shear Layer Entrainment," *AIAA Journal*, Vol. 24, No. 11, 1986, pp. 1791–1796. doi:10.2514/3.9525

[18] Freund, J. B., and Wei, M., "Some Small Changes That Make a Mixing Layer Very Quiet," AIAA Paper 2005-0997, Jan. 2005.

[19] Rennie, R. M., Siegenthaler, J. P., and Jumper, E. J., "Forcing of a Two-Dimensional, Weakly-Compressible Subsonic Free Shear Layer," AIAA Paper 2006-0561, Jan. 2006.

[20] Wygnanski, I., and Oster, D., "The Forced Mixing Layer Between Parallel Streams," *Journal of Fluid Mechanics*, Vol. 123, 1982, pp. 69. doi:10.1017/S0022112082002961

X. Zhong
Associate Editor